Insulin-like Growth Factor 2 Is Required for Progression to Advanced Medulloblastoma in *patched1* Heterozygous Mice

Ryan B. Corcoran, Tal Bachar Raveh, Monique T. Barakat, Eunice Y. Lee, and Matthew P. Scott

Departments of Developmental Biology, Genetics, and Bioengineering, Howard Hughes Medical Institute, Stanford University School of Medicine, Stanford, California

Abstract

Medulloblastoma (MB) can arise in the cerebellum due to genetic activation of the Sonic Hedgehog (Shh) signaling pathway. During normal cerebellum development, Shh spurs the proliferation of granule neuron precursors (GNP), the precursor cells of MB. Mutations in the Shh receptor gene *patched1* (*ptc1*+/−) lead to increased MB incidence in humans and mice. MB tumorigenesis in mice heterozygous for *ptc1*+/− shows distinct steps of progression. Most *ptc1*+/− mice form clusters of preneoplastic cells on the surface of the mature cerebellum that actively transcribe Shh target genes. In ~15% of mice, these preneoplastic cells will become fast-growing, lethal tumors. It was previously shown that the loss of function of insulin-like growth factor 2 (*igf2*) suppresses MB formation in *ptc1*+/− mice. We found that *igf2* is not expressed in preneoplastic lesions but is induced as these lesions progress to more advanced MB tumors. *Igf2* is not required for formation of preneoplastic lesions but is necessary for progression to advanced tumors. Exogenous Igf2 protein promoted proliferation of MB precursor cells (GNP) and a MB cell line, PZp53^{MED}. Blocking *igf2* signaling inhibited growth of PZp53^{MED} cells, implicating *igf2* as a potential clinical target. [Cancer Res 2008;68(21):8788–95]

Introduction

Mutations in the Sonic hedgehog (Shh) signaling pathway that cause constitutive Shh target gene transcription are associated with the formation of many human tumors. Medulloblastoma (MB), the most common malignant brain tumor in children, can arise when such mutations occur in developing cerebellar granule neuron precursors (GNP; ref. 1). Loss of function of the *PATCHED1* (*PTCH, ptc1* in mice) tumor suppressor gene, which occurs in sporadic and hereditary MB, is the most common of these mutations (2, 3). *PTCH* encodes a 12-transmembrane receptor (Ptc1) for Shh. In the absence of Shh signal, Ptc1 inhibits the downstream transducers of the Shh pathway, preventing activation of target gene transcription by Gli transcription factors. Shh activates target gene transcription by binding to and inhibiting Ptc1. Shh and Ptc1 are therefore antagonists. *Ptc1* and *gli1* are Shh target genes. Induction of *ptc1* and *gli1* by Shh creates a negative feedback loop (through Ptc1) that restrains ongoing Shh signaling and a positive feedback loop (through Gli1) that acts as an amplifier of the initial Shh signal. The balance between negatively acting Ptc1 and positively acting Gli proteins determines the functional state of Shh pathway activity (4–7).

In the developing cerebellum, Shh signal produced by Purkinje neurons stimulates proliferation of GNPs in the external germinal layer (EGL) on the surface of the cerebellum (8–10). Shh target genes, such as *N-myc* and *cyclin-D1*, become active and promote cell cycle entry (11–13). In mice, expansion of GNPs ceases within 3 weeks after birth, as GNPs migrate to the internal granule cell layer and differentiate to form mature granule neurons (Fig. 1*A*). By the end of this period, the EGL has disappeared.

Mice heterozygous for *ptc1* spontaneously form MB and rhabdomyosarcoma (RMS), a tumor derived from muscle (14, 15). These tumors exhibit constitutive Shh target gene expression due to reduced Ptc1 activity. Small molecule Shh pathway inhibitors can reduce tumor formation in *ptc1*+/− mouse models of MB (16, 17), demonstrating the dependence of MB cells on Shh target gene expression. Therefore, knowledge of critical Shh target genes or genes that cooperate with the Shh pathway to promote tumorigenesis has potential clinical importance as a step toward identifying drug targets.

Insulin-like growth factor 2 (*igf2*) is expressed at high levels compared with normal tissue in both MB and RMS in *ptc1*+/− mice (15) and in humans (18–20, 22). Hahn and colleagues (21) showed that *igf2* is critical for the formation of both MB and RMS in *ptc1*+/− mice. When *ptc1*+/− mice are crossed into an *igf2*-deficient background, they no longer form MB or RMS such as their *igf2*-wild-type littermates. *Igf2* has also been shown to synergize with the Shh pathway to promote MB, as retroviral transfer of Shh and Igf2 expression constructs into postnatal cerebella causes a higher incidence of MB formation than delivery of a Shh expression construct alone (23). Igf2 protein can stimulate proliferation of cultured MB cell lines and their precursor cells, GNPs, suggesting a mechanistic basis for the role of *igf2* in MB tumorigenesis (24).

Important questions remain about the involvement of *igf2* in MB. The mechanism of increased *igf2* expression in MB and RMS from *ptc1*+/− mice is not clear. Two independent analyses of *igf2* expression from maternal and paternal alleles showed that increased *igf2* levels do not result from loss of imprinting in MB or RMS or from gene amplification (21, 24). Rather, increased *igf2* RNA levels seemed to be induced at a purely transcriptional level. Hahn and colleagues (21) proposed that *igf2* might be a Shh target gene, overexpressed in *ptc1*+/− tumors due to constitutive Shh pathway target gene transcription. In support of this hypothesis, the authors showed that compared with *ptc1*+/+ embryonic day 8.5 embryos, *igf2* transcript levels were higher in *ptc1*+/− embryos and highest in *ptc1*−/− embryos. C3H/10T1/2 cells transfected with the Shh pathway–activating transcription factor Gli1 have increased *igf2* RNA levels after 72 hours (25). However, cultured GNPs treated with Shh do not have increased *igf2* RNA levels at the 6-hours time point tested (24). Therefore, it remains unclear

Requests for reprints: Matthew P. Scott, Howard Hughes Medical Institute, Clark Center W252, 318 Campus Drive, Stanford University School of Medicine, Stanford, CA 94305. Phone: 650-725-7680; Fax: 650-725-2952; E-mail: mscott@stanford.edu.
©2008 American Association for Cancer Research.
doi:10.1158/0008-5472.CAN-08-2135

whether constitutive Shh pathway transcriptional activity causes the increased levels of *igf2* transcript found in MB.

It is also not clear what role *igf2* plays in MB tumorigenesis. *Igf2* could contribute to tumor initiation, either as a critical Shh target gene or an independently regulated gene. Alternatively, *igf2* could cooperate with the Shh pathway to cause tumor progression at a specific stage of tumorigenesis.

Here, we evaluate *igf2* expression at multiple stages of MB tumorigenesis. We also test the requirement for *igf2* during early and late stages of tumorigenesis. We show that *igf2* is not required for tumor initiation but is required for progression to advanced MB lesions. Modulation of *igf2* signaling can regulate proliferation of MB cells *in vitro*, suggesting that *igf2* is important not just for tumor progression but also for tumor maintenance.

Materials and Methods

Mouse strains. *Igf2* knockout mice were kindly provided by Dr. Argiris Efstratiadis (Columbia University, New York, NY). Because *igf2* is an imprinted gene for which only the paternal gene is expressed, male mice heterozygous for *igf2* were mated with *ptc1*+/− mice (108B2; ref. 14) with or without the *Math1-gfp* transgene. *Math1-gfp* mice were kindly provided by Dr. Jane Johnson (University of Texas Southwestern Medical Center, Dallas, TX). Offspring heterozygous for the *igf2* knockout allele by PCR, using primers specific for wild-type and mutant *igf2* alleles, were effectively *igf2* null. Offspring homozygous for the wild-type *igf2* allele were considered wild-type.

Math1-gfp ptc1+/− *igf2*− mice and *igf2*+ littermates were sacrificed at 3 wk to evaluate for early MB formation. Cerebella were visualized under a fluorescent dissecting microscope for development of green fluorescent protein (GFP)-positive lesions. Adult *ptc1*+/− *igf2*− and *ptc1*+/− *igf2*+ littermates were assessed for MB formation at 20 to 24 wk by visual inspection of cerebella and X-gal staining, as previously described (14).

Microarray analysis. Early and intermediate MB cells were isolated from cerebella of *math1-gfp ptc1*+/− mice at 3 to 6 wk or 10 to 20 wk, respectively. Tumors were identified by inspection of cerebella for GFP fluorescence. Tumors were dissected and GFP-expressing cells were isolated by fluorescence-activated cell sorting (FACS). Advanced MBs were isolated from symptomatic *ptc1*+/− mice and tumor cells were purified as previously described (10). RNA was isolated using Trizol reagent (Life Technologies). RNA was amplified using Riboamp kit (Arcturus). Probe was reverse transcribed in the presence of aminoallyl-dUTP (Sigma) and subsequently labeled with Cy3 or Cy5 dye (Amersham). Probe made from tumor cell RNA was hybridized to cDNA microarrays produced by the Stanford Microarray Facility. Cy3-labeled tumor cell probes were hybridized against Cy5-labeled probe made from RNA isolated from high-level GFP-expressing GNPs isolated by FACS from the outer EGL of *math1-gfp* mice. *Igf2* transcript level values are displayed relative to outer EGL GNPs. Average values of five independent probes were determined, per experiment.

Quantitative real-time reverse transcription-PCR. *Igf2* and *gli1* transcript levels were measured by real-time PCR using RNA isolated with Trizol reagent (Life Technologies). Gene expression assays for mouse *igf2*, *gli1*, and *pgk1* and *gapdh* were purchased from Applied Biosystems. *Igf2* and *gli1* transcript levels were normalized to *gapdh* transcript levels in tumor cell, fibroblast, and PZp53^{MED} cell experiments and to *pgk1* transcript levels in GNP cell experiments.

P7 GNPs were isolated and cultured with or without 3 μg/mL Shh for 48 h as previously described (10). PZp53^{MED} cells, *ptc1*+/− fibroblasts, or *ptc1*+/+ fibroblasts were cultured to confluence in DMEM + 0.5% fetal bovine serum (FBS) in the presence or absence of 10 μmol/L cyclopamine. RNA from *ptc1*+/+ fibroblasts transfected with cytomegalovirus (CMV) promoter–driven GFP, Gli1, and Gli2 expression constructs was kindly provided by Dr. Anna Penn (Stanford University, Stanford, CA).

***In situ* hybridization studies.** ^{35}S-UTP–labeled probes were made by *in vitro* transcription, with T3 or T7 RNA polymerase, of linearized plasmids purchased from American Type Culture Collection. Probes were diluted to 5×10^6 cpm/mL final concentration in buffer containing Escherichia coli tRNA and DTT. Frozen tissue was embedded in ornithine carbamyl transferase and cut to 15-μm sections on glass slides. Sections were dried and fixed with 4% paraformaldehyde and dehydrated through ethanol. Before hybridization, sections were treated with Proteinase K, acetylated with acetic anhydride, and dehydrated through ethanol. Hybridization was performed at 60°C to 65°C overnight. Sections were RNase treated and washed with increasing stringencies of SSC with DTT. Slides were dehydrated, dipped in photographic emulsion, incubated for 4 to 14 d, developed, and counterstained with Cresyl violet.

Cell survival assays. P7 GNPs were cultured in Neurobasal medium (Life Technologies) with or without B27 supplement for 48 h. Igf2 protein (R&D systems) was added to a final concentration of 250 ng/mL. Cell titer was determined with CellTiter96 assay (Promega).

Cell proliferation assays. Proliferation of PZp53^{MED} cells in the presence of anti-Igf1R (Anti-IR3; Calbiochem) blocking antibody was assayed by seeding cells at 1 to 2×10^3 cells per well of a 96-well plate in DMEM+0.5% FBS. Antibody or Igf2 protein was diluted in DMEM+0.5% FBS and added to cells 3 h after seeding. Cells were cultured for 48 h, and cell titer was determined by CellTiter96 assay.

For sIgf2R experiments, PZp53^{MED} cells were seeded at 6×10^3 cells per well on coverslips in 24-well plates. The next day, cells were cotransfected in triplicate with 0.5 μg pEYFP-N3 and 1 μg of either pEFBOS-sIgf2R (kindly provided by Dr. Bass Hassan, University of Oxford, Oxford, United Kingdom) or, as a control, 1 μg of pECFP-N2. Twenty-four hours posttransfection, cells were switched to DMEM+0.5% FBS and cultured for an additional 36 h. BrdUrd was added for the final 6 h. Cells were fixed, permeabilized, blocked, and DNase treated as above. Cells were stained with rat anti-BrdUrd antibody (Abcam) at 1:50 dilution. The next day, anti-BrdUrd staining was detected with TRITC-conjugated anti-rat secondary antibody. Percentage of YFP-positive cells that were also BrdUrd positive was calculated for each sample.

Immunoblotting and immunoprecipitation. Cells were grown to confluence in 10-cm plates and then serum starved for 48 h in DMEM+0.5% FBS. Then, cells were treated with 1 μg/mL or 10 μg/mL anti-Igf1R antibody (Calbiochem) and/or 250 ng/mL Igf2 protein (R&D systems), as described above, for 30 min. Protein extracts were prepared in radioimmunoprecipitation assay buffer containing 50 mmol/L Tris, 1% NP40, 0.25% sodium deoxycholate, 150 mmol/L NaCl, 1 mmol/L EDTA, 1 mmol/L DTT, 1 mmol/L phenylmethylsulfonyl fluoride, protease inhibitors (Roche), and phosphatase inhibitors (Calbiochem). Protein samples (30 μg per sample) were resolved by SDS-PAGE, transferred onto polyvinylidene difluoride membranes (Bio-Rad), and then immunoblotted with the following antibodies: anti-Igf1Rβ (Santa Cruz Biotechnology), anti–phospho-Akt (ser473; Cell Signaling), anti-Akt (Cell Signaling), and anti–β-Tubulin (Covance). For determination of Igf1R phosphorylation, 200 μg protein extracts were incubated overnight at 4°C with anti-phosphotyrosine antibody (Upstate) bound to protein G beads (Invitrogen). The immunoprecipitates were washed extensively, eluted in SDS sample buffer, and subjected to Western blotting analysis using an anti-Igf1Rβ antibody (Santa Cruz Biotechnology).

Results

***Igf2* transcription increases at a late stage of MB tumorigenesis.** To observe developing MBs, we crossed *ptc1*+/− mice with mice expressing GFP from a *Math1* enhancer that is specifically expressed in immature GNPs (26). *Math1* is a critical regulator of GNP development that is required for the formation of GNPs (27). Because *Math1* expression is preserved throughout MB tumorigenesis (28, 29), tumor cells from multiple stages of MB progression could be readily detected and isolated by virtue of their GFP expression. RNA from these cells was analyzed using cDNA microarrays to identify changes in gene expression that occur at each stage of MB tumorigenesis. We collected three tumor cell

populations for this analysis (Fig. 1*A*): (*a*) preneoplastic "early" MB lesions that are present in >85% of 3-week-old mice, the majority of which regress by 6 weeks; (*b*) intermediate, asymptomatic MB lesions that are present in ~15% of 10-week-old mice, the majority of which seem to progress to advanced MBs; and (*c*) advanced, symptomatic MB that occur in ~15% of mice, with peak incidence at ages ~20 weeks. For comparison, we used RNA from a purified population of GNPs, the precursor cells of MB, isolated from the EGL of normal postnatal day 7 (P7) cerebella.

We found that *igf2* transcript levels are not significantly increased in early MB lesions relative to normal GNPs. *Igf2* transcript levels are significantly increased only in intermediate MBs and are even higher in advanced MBs (Fig. 1*B*). Only 20% of individually tested early MBs have significantly increased levels relative to normal GNPs, compared with 36% of intermediate and 100% of advanced MBs (Fig. 1*C*). To confirm these microarray results, *igf2* transcript levels from individual early, intermediate, and advanced MBs were measured by quantitative real-time PCR. Advanced MB samples showed a statistically significant increase (~20- to 50-fold) in *igf2* transcript levels (Fig. 1*D*). *Igf2* transcript levels were not statistically increased in any of the early or intermediate MBs tested. Increased *igf2* transcription seems to be a late event in MB tumorigenesis and is correlated with the critical transition from early and intermediate to advanced MBs.

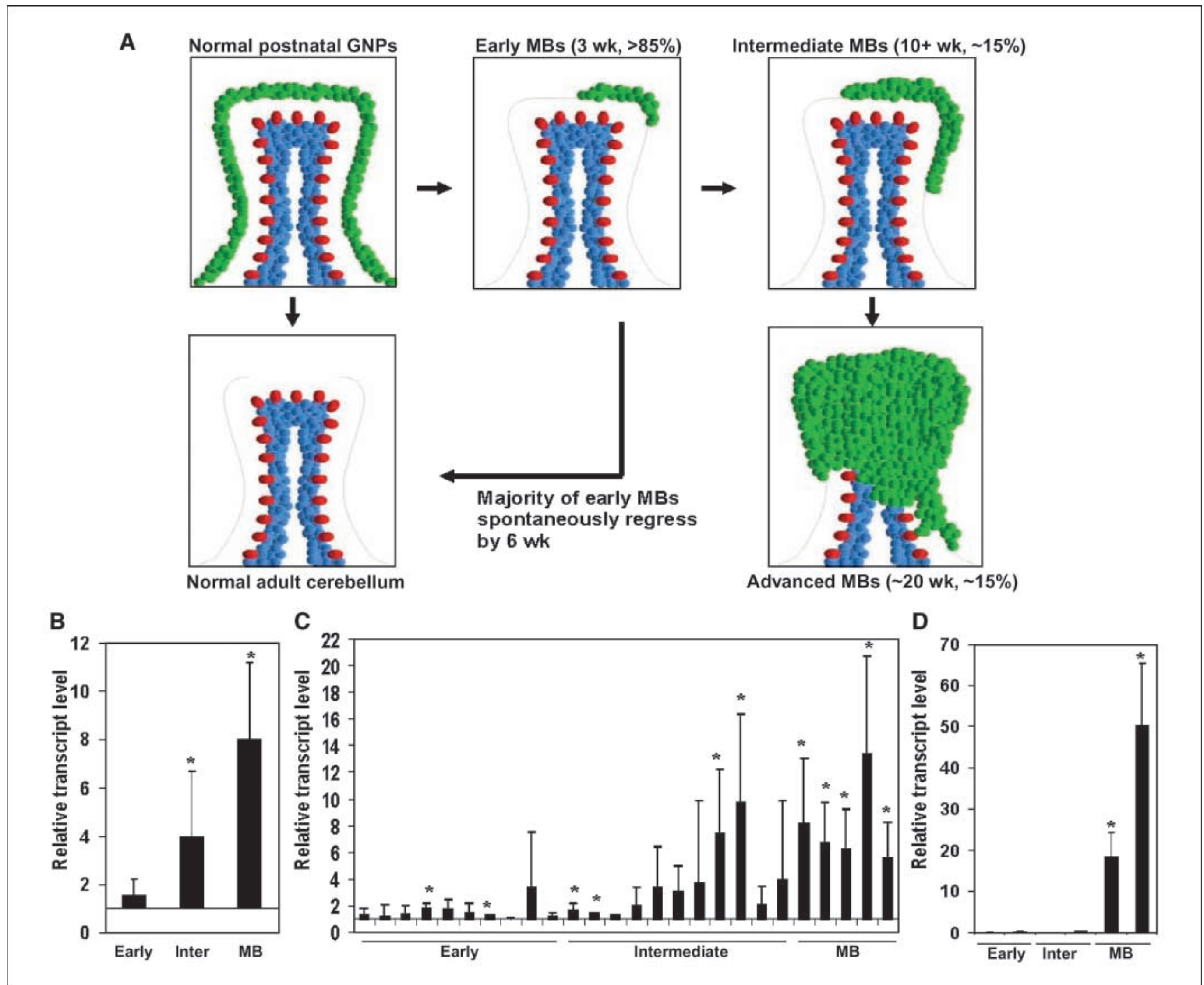

Figure 1. *Igf2* transcription increases at a late stage of MB tumorigenesis. *A,* multiple stages of MB tumorigenesis in the *ptc1*+/− mouse. GNPs (*green*) in the normal developing postnatal cerebellum proliferate in response to Shh produced by underlying Purkinje cell neurons (*red*). Throughout the first 3 wk of postnatal life, GNPs stop responding to Shh, differentiate, and migrate into the internal granule cell layer to become mature granule neurons (*blue*). GNPs express *Math1*, whereas mature granule neurons do not. From age 3 wk to adulthood, no GNPs remain in the normal cerebellum, and *Math1* expression is lost. However, in the majority of *ptc1*+/− mice (>85%) at age 3 wk, small clusters of *Math1*-expressing GNP-like cells persist as early, preneoplastic MB lesions. The majority of these lesions regress spontaneously by age 6 wk. A subset of these lesions (~15% of total) progress to form more aggressive-appearing intermediate, asymptomatic MBs by 10 wk and eventually advanced, symptomatic MBs by age ~20 wk. *B,* pooled averages of *igf2* transcript levels by microarray analysis of preneoplastic early MBs (*early*), intermediate MBs (*inter*), and advanced MBs (*MB*). Values are relative to normal P7 GNPs. Note that *igf2* transcript levels are not increased until late in tumorigenesis. *, $P < 0.01$. *C,* fold-enrichment of *igf2* transcript in individual MB lesions relative to normal GNPs. Each measurement is the average of five different *igf2* probes. *, $P < 0.05$. *D,* quantification of *igf2* transcript levels by quantitiative real-time PCR from individual early MBs, intermediate MBs, and advanced MBs. Values are relative to normal P7 GNPs. *, $P < 0.01$. *Columns,* mean; *bars,* SD (*B-D*). *P* values were calculated using Student's *t* test relative to normal P7 GNP controls.

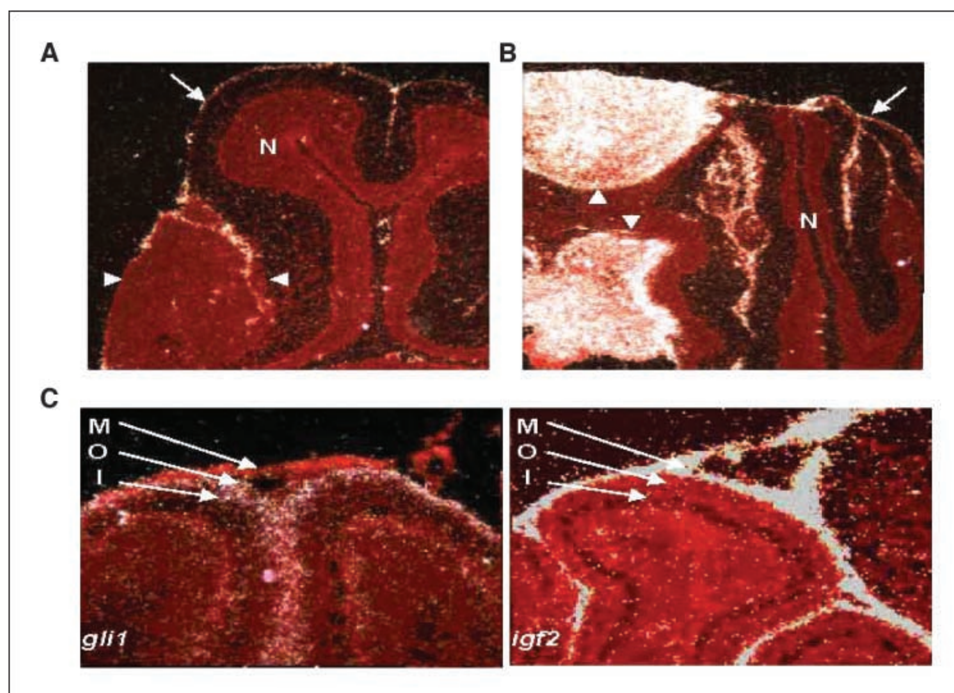

Figure 2. Expression of *igf2* in developing cerebella and MB. *A* and *B, in situ* hybridization studies of early MB (*A*) and advanced MB (*B*) using a probe specific to *igf2*. Signal from hybridized probe seems white. Tissue is counterstained in red. In each panel, tumor is outlined by arrowheads. *Igf2* transcript is not seen in early MB (*A*) but is seen at high levels in the advanced MB (*B*). *Igf2* transcript is not seen in normal cerebellum (*N*) but is observed in the meninges (*arrows*) surrounding the cerebellum. *C, in situ* hybridization studies of P7 cerebella using probes specific to *igf2* or *gli1*. *Igf2* transcript is observed in the meninges (*M*) but not in the outer (*O*) or inner (*I*) EGL. Conversely, the Shh target transcript *gli1* is absent from the meninges but is seen in the outer, but not inner EGL.

In situ hybridization of early and advanced MB with a probe specific for *igf2* showed absent or low levels of *igf2* transcript in early MB but very high levels of transcript in advanced MBs (Fig. 2*A* and *B*). These data are consistent with our microarray data, confirming that increased *igf2* transcription is a late event in MB tumorigenesis. High levels of *igf2* transcript were also detected in the meninges of normal cerebella and cerebella containing tumors (Fig. 2*A* and *B, arrows*; Fig. 2*C*).

***Igf2* transcription can be regulated by the Shh pathway.** The temporal pattern of *igf2* expression during MB tumorigenesis raises the question of how the induction of *igf2* expression is regulated. The expression pattern of *igf2* is different from what is expected and observed for most Shh target genes. Shh target genes such as *ptc1* and *gli1* are typically expressed at high levels in GNPs of the outer EGL, which proliferate in response to Shh produced by Purkinje neurons. *In situ* hybridization studies of developing P7 cerebella show high levels of *igf2* transcript in the meninges and low levels in the EGL (Fig. 2*C*). Conversely, *gli1*, a Shh target gene in all tissues, is absent from the meninges but abundantly transcribed in the outer EGL. We conclude that *igf2* transcript is minimally produced in areas of Shh target gene transcription in the developing cerebellum.

To further investigate the relationship between Shh pathway activity and *igf2* transcription, we examined the effect on *igf2* transcript levels of activating or inhibiting the Shh pathway in cultured GNPs and MB cells. Shh-treatment of primary GNP cultures does not increase *igf2* transcript levels after 6 hours (24). However, treatment of GNPs with Shh for 24 hours increased *igf2* transcription relative to untreated controls (Fig. 3*A*). Similarly, treatment of PZp53^{MED} cells, a MB cell line derived from a *ptc1*+/− *p53*−/− mouse MB, with the Shh pathway inhibitor, cyclopamine reduced *igf2* transcript levels relative to untreated controls (Fig. 3*B*). These results show that activation or inhibition of Shh target gene transcription can influence *igf2* mRNA levels in cultured MB cells and their precursors.

Igf2 also behaves as a Shh-responsive gene in fibroblasts derived from *ptc1*+/+ or *ptc1*+/− embryos. When *ptc1*+/+ fibroblasts are transfected with Shh target gene–activating transcription factors *gli1* or *gli2, igf2* transcription is induced >1,500-fold (Fig. 3*C*). *Ptc1*+/− embryos have reduced Ptc1 function and exhibit increased transcription of Shh target genes compared with *ptc1*+/+ embryos (14). Fibroblasts derived from *ptc1*+/− embryos have a 4-fold higher basal level of *igf2* transcription than *ptc1*+/+ embryonic fibroblasts (Fig. 3*D*). Cyclopamine treatment does not change *igf2* transcript levels in *ptc1*+/+ fibroblasts but decreases *igf2* transcript levels in *ptc1*+/− fibroblasts to levels similar to those seen in *ptc1*+/+ fibroblasts.

In summary, regulation of *igf2* by the Shh pathway is complex. Although *igf2* is a Shh-responsive gene in some cell types, it seems that *igf2* is refractory to induction by Shh in the developing cerebellum and in early MBs that express other Shh target genes.

***Igf2* is required for MB tumor progression but not tumor initiation.** Hahn and colleagues (21) showed that *igf2* is required for formation of advanced MBs in *ptc1*+/− mice, but which stage of tumorigenesis requires *igf2* is unknown. Because *igf2* transcription is induced during the transition between early and advanced MBs, we tested whether *igf2* is required for early MB formation. The low level of *igf2* expression in early MBs suggests that early MB formation would not require *igf2* to be active within the pretumor cells. However, it is still possible that *igf2* might play a role in early MB tumor initiation because paracrine Igf2 signal produced in the neighboring meninges could stimulate GNPs or MB cells during early tumorigenesis. In this way, early lesions might be dependent on *igf2*, despite their lack of *igf2* expression. Late in tumorigenesis, when lesions become too large to subsist on meningeal Igf2 alone, Igf2 produced by the tumor cells themselves may supplement the meningeal source through autocrine signaling.

To distinguish between these possibilities, we crossed *Math1-gfp ptc1*+/− females with *igf2*+/− males and analyzed *Math1-gfp*

ptc1+/− offspring that were *igf2*+/− or *igf2*+/+. Because *igf2* is an imprinted gene, only the paternal allele is expressed, and *igf2*+/− offspring are effectively *igf2* null. We analyzed *igf2*+/− and *igf2*+/+ mice for early MB lesions and for MB formation. Consistent with previously reported results (21), no advanced MBs were observed in *igf2* null offspring, whereas advanced MBs formed as expected in their *igf2* wild-type littermates (Table 1). In contrast, formation of early MB lesions occurred even in the absence of *igf2*. All *igf2* wild-type and null offspring developed clusters of preneoplastic cells by ages 3 weeks. These results suggest that *igf2* plays a critical role exclusively in the progression to advanced MBs.

Inhibition of *igf2* signaling reduces proliferation of MB cells. *Igf2* could act at a specific point in the tumor progression decision or as an ongoing promoter of growth. We tested whether *igf2* plays a role in maintaining the growth of fully developed MB cells. Proliferative and survival-promoting signals are important for maintaining tumor growth. It was shown previously that Igf2 protein can induce proliferation in GNPs (24). Similarly, we find that Igf2 increases the fraction of proliferating GNPs 3-fold (Fig. 4*A*). We also show that Igf2 promotes cell survival of cultured GNPs. If GNPs are cultured in minimal medium, the majority undergoes apoptosis. GNPs cultured in minimal medium with Igf2 alone show enhanced survival similar to GNPs grown in fully supplemented medium (Fig. 4*B*).

We tested the effects of augmenting or inhibiting *igf2* signaling on cell proliferation of the MB cell line, PZp53^{MED}. Addition of exogenous Igf2 increased proliferation of MB cells in a dose-dependent manner (Fig. 5*A*).

Igf2 ligand acts through the Igf1 receptor (Igf1R), which also can serve as a receptor for Igf1 and Insulin. We used an Igf1R-blocking antibody to inhibit the autocrine activity of endogenously produced Igf2. PZp53^{MED} cells derived from a MB have low basal levels of Igf1R phosphorylation and phosphorylation of Igf pathway target Akt (Fig. 5*B*). Phosphorylation of Igf1R and Akt increased dramatically when treated with exogenous Igf2 protein. In contrast, only a minimal increase in phosphorylation was observed in Igf2-treated HELA cell controls. When cells were treated with anti-Igf1R antibody and Igf2, levels of Igf1R and Akt phosphorylation are reduced to levels equal to or below baseline. Treatment of PZp53^{MED} cells with anti-Igf1R antibody can therefore block the effects of even superphysiologic levels of Igf2.

When PZp53^{MED} cells or HELA cell controls were cultured in the presence of anti-Igf1R antibody, PZp53^{MED} cells showed a ∼40% decrease in cell number relative to untreated PZp53^{MED} cells after 48 hours (Fig. 5*C*). There was no significant difference in cell number between treated and untreated HELA cells.

Blocking Igf1R can potentially also block the effects of Igf1 and Insulin. To more specifically block the effects of MB cell–produced Igf2, we used a soluble Igf2-Receptor (sIgf2R) construct that has been used previously to block the effects of Igf2 on cells or *in vivo* tissues (30, 31). When sIgf2R is expressed, it is secreted from the cell where it binds and sequesters the Igf2 ligand, blocking its effect. Because sIgf2R specifically binds Igf2, it does not interfere with the actions of insulin, Igf1, or Igf1R. When PZp53^{MED} cells were transfected with sIgf2R, they showed a ∼60% reduction in proliferation, measured by BrdUrd incorporation, relative to CFP-transfected cells (Fig. 5*D*). These results indicate that Igf2 is specifically required for MB cell proliferation. In summary, we observe that activation or inhibition of Igf2 signaling can promote or prevent MB cell growth, respectively.

Discussion

The mechanism of *igf2* induction in MB. Here, we present evidence that *igf2* is a Shh-responsive gene in cultured GNPs, MB cells, and fibroblasts. It might seem that *igf2* is expressed at high levels in MBs because these tumors have increased Shh target gene transcription. However, increased *igf2* transcription is not seen until late stages of MB tumorigenesis, although constitutive Shh target gene transcription begins at early stages. Furthermore, increased *igf2* transcription is not seen in developing GNPs of the outer EGL *in vivo* (Fig. 2*B*), which respond to Shh signal and express Shh target genes (10). Previous studies have indicated that neither genomic imprinting nor gene amplification are the causes of increased *igf2* expression (21, 24). Rather, increased *igf2* transcription seems to be due purely to transcriptional regulation.

One explanation for why *igf2* transcription might be induced by Shh in cultured GNPs but not in GNPs or early tumor cells *in vivo* is that the level of Shh pathway activation achieved in culture may be higher than *in vivo*. The concentration of Shh protein used in our cultured assays causes maximal activation of Shh target gene transcription (10). If *igf2* transcription requires very high levels of Shh pathway activity, then perhaps this threshold activity is not achieved until late in tumorigenesis. Alternatively, the presence of some activating factor in the culture medium, or the absence of some inhibitory factor that is present in the intact developing cerebellum may account for the differences in the response of GNPs to Shh *in vitro* versus *in vivo*. For example, restrictive chromatin

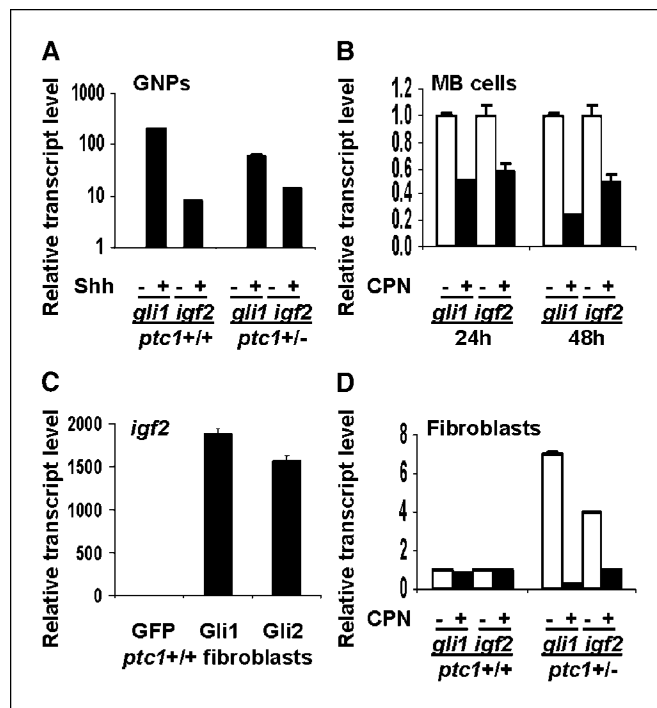

Figure 3. *Igf2* transcription can be regulated by the Shh pathway. *A,* levels of *gli1* and *igf2* transcript are increased in *ptc1*+/+ or *ptc1*+/− P7 GNPs treated with Shh (3 μg/mL) for 48 h. *B,* PZp53^{MED} cells (*MB cells*) show decreased levels of *gli1* and *igf2* transcript when treated with the Shh pathway inhibitor cyclopamine (*CPN*) for 24 or 48 h. *C, ptc1*+/+ fibroblasts transfected with CMV promoter–driven Gli1 or Gli2 expression constructs showed increased levels of *igf2* transcript after 24 h compared with cells transfected with a GFP control. *D, ptc1*+/− fibroblasts have increased levels of *gli1* and *igf2* transcript at baseline. In cyclopamine-treated *ptc1*+/− fibroblasts, levels of both transcripts are reduced to levels comparable with those seen in *ptc1*+/+ fibroblasts. *Columns,* mean; *bars,* SD.

Table 1. Early MB formation persists in *Math1-gfp ptc1+/− igf2−* mice

	ptc1+/− igf2+	*ptc1+/− igf2−*
Early MBs	3/3	3/3
Advanced MBs	5/18	0/12

NOTE: One hundred percent of *ptc1+/− igf2+* and *ptc1+/− igf2−* mice sacrificed at age 3 wk had early MB lesions. However, although *ptc1+/− igf2+* mice developed advanced MBs, no MBs were observed in *ptc1+/− igf2−* mice ($P < 0.05$).

structure or the presence of repressive transcription factors in cells *in vivo* may not be reproduced when these cells are cultured *in vitro*.

Another explanation for the pattern of *igf2* regulation could be that Shh target gene transcription alone cannot account for increased *igf2* transcription in MB. Shh target gene transcription likely plays a role in increased *igf2* transcription because *igf2* transcript levels are decreased in cultured MB cells treated with the Shh pathway inhibitor cyclopamine, albeit only 2-fold. Another regulator may cooperate with the Shh pathway to induce *igf2* transcription.

What might be responsible for the dramatic increase in *igf2* transcription that occurs late in MB tumorigenesis? Increased *igf2* expression due to altered transcriptional regulation in human tumors is a common finding, and perhaps such a mechanism cooperates with the Shh pathway to cause increased *igf2* transcript levels in MB. *Igf2* expression is induced by overexpression of the early growth response gene 1 protein in prostate cancer (32). *Igf2* expression may be induced due to mutation of its flanking regulatory sequences. Changes in the 3′ untranslated region of *igf2* are associated with 100- to 1,000-fold increases in *igf2* transcript levels in colorectal cancer (33). Altered methylation of the *igf2* promoter causes increased *igf2* transcription in hepatoblastoma (34).

PTEN activity can modulate *igf2* expression in hepatoma (35). Increased PTEN activity leads to decreased *igf2* transcription, and decreased PTEN activity causes increased *igf2* transcription. Because *igf2* signaling antagonizes PTEN activity by activating PI3-K (36), increases in Igf2 production may induce progressively increased autotranscription in feed-forward fashion. This hypothesis could explain why Hartmann and colleagues (24) did not see induction of *igf2* transcription in GNPs treated with Shh alone for 6 hours but did see low-level induction of *igf2* transcription in GNPs treated with Shh and Igf2. Shh target gene transcription and Igf2 production, first from the meninges and later from tumor cells themselves, may cooperate to induce *igf2* transcription during MB tumorigenesis. A better understanding of the mechanism of increased *igf2* expression in MB could yield opportunities to reverse this induction and inhibit the oncogenic effects of Igf2.

Temporal requirement for *igf2* in late tumorigenesis. Our results suggest that induction of *igf2* transcription is a late event in MB tumorigenesis that occurs as the preneoplastic cells of early MBs acquire a malignant phenotype. The requirement for Igf2 activity arises in late tumorigenesis, as early MB lesion formation occurs in the absence of *igf2*. These data do not preclude that *igf2* may contribute to early tumorigenesis, as high levels of *igf2* transcription are observed in the overlying meninges. However, the indispensable role for *igf2* in MB formation occurs only in the late malignant conversion of MB and not during tumor initiation. This hypothesis is consistent with the observation that activation of Igf2 signaling alone in the developing cerebellum by retroviral transfer of *igf2* is not sufficient to initiate MB formation (23).

This temporal pattern suggests a cooperation of autocrine Igf2 and other Shh target genes in MB tumorigenesis. Recent data have supported a cooperative hypothesis for these pathways. If Shh and Igf2 are introduced into neural progenitors by retroviral delivery, the frequency of MB formation is 3-fold greater than with delivery of Shh alone (23). The Shh and Igf2 pathways converge to trigger the production of high levels of N-myc protein. The Shh pathway stimulates transcription of *N-myc*, whereas the Igf pathway leads to stabilization of N-myc protein through Akt-mediated effects on GSK-3β (12, 13, 37). Consistent with this hypothesis, retroviral delivery of stabilized N-myc along with Shh also causes a 3-fold increase in MB frequency compared with Shh alone (38).

Igf2 might also cooperate with the Shh pathway in MB tumorigenesis by activating cell survival pathways. We show that Igf2 can promote GNP survival under conditions that normally lead to apoptosis. Similarly, the Igf family members, insulin and Igf1, can promote survival in cultured GNPs, likely through activation of the proto-oncogene Akt (39).

Igf2 may cooperate with Shh to promote transcription of Shh target genes. Transcription of the Shh target genes, *gli1* and *cyclinD1*, is significantly increased in GNPs cotreated with Shh and Igf2 compared with Shh alone (24). Igf2 could increase levels of Shh target transcripts, including, as proposed earlier, *igf2* itself, to promote tumor formation.

A model for MB tumorigenesis. Based on our findings, we propose the following model of MB tumorigenesis. Normal GNPs in *ptc1+/−* mice accumulate one or more mutations that result in constitutive Shh target gene expression. The mutation could inactivate the remaining copy of *ptc1*, perhaps by methylation (16), or affect some other component. Cells with active Shh targets would proliferate and would resist cues to arrest and differentiate,

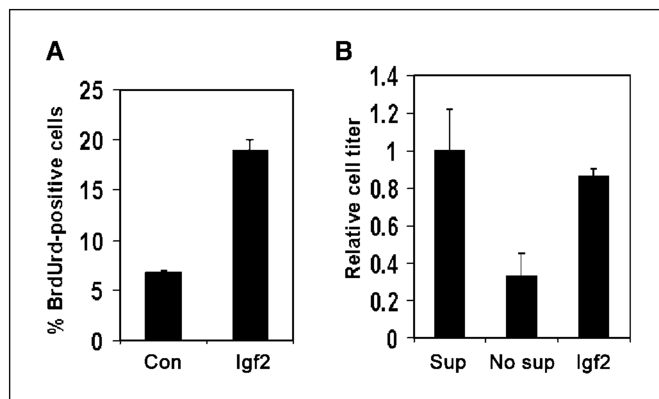

Figure 4. Igf2 promotes GNP proliferation and survival. *A,* the percentage of GNPs which are proliferating (measured by BrdUrd staining) is increased when cells are cultured in the presence of Igf2 versus control (*con*) for 48 h. *B,* Igf2 increases GNP survival under conditions which normally lead to apoptosis. If P7 GNPs are cultured in media without supplement (*no sup*) for 48 h, a majority undergo apoptosis compared with those cultured in supplemented media (*sup*). When Igf2 is added to unsupplemented medium, GNP survival is restored. *Columns,* mean; *bars,* SD.

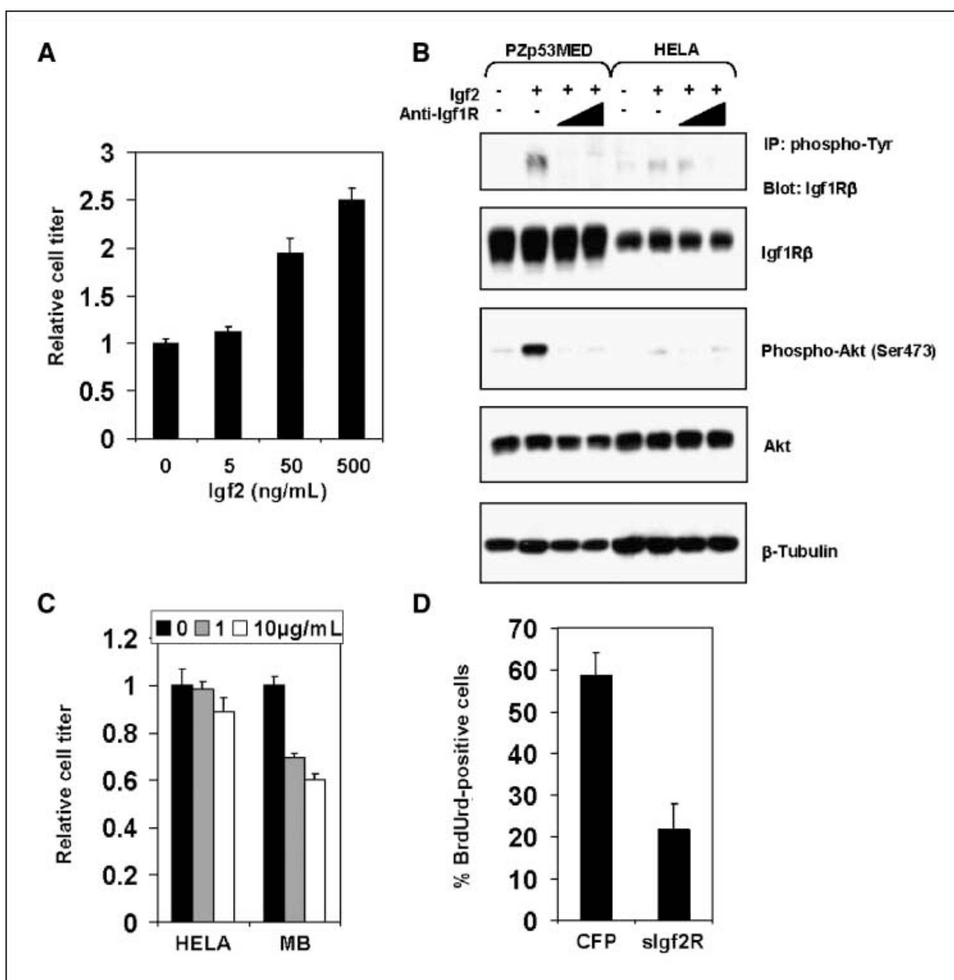

Figure 5. Inhibition of Igf2 signaling reduces MB cell proliferation. *A,* proliferation of PZp53^{MED} cells is increased in a dose-dependent manner by exogenous Igf2 protein. Cell titer was measured after 48 h in culture. *B,* levels of Igf1R and Akt phosphorylation in PZp53^{MED} and HELA cell controls treated for 30 min with Igf2 with or without increasing concentrations of an antibody that blocks the Igf1R (anti-Igf1R; 1 μg/mL; 10 μg/mL). Levels of Igf1R and Akt phosphorylation increase dramatically in PZp53^{MED} cells and only minimally in HELA cells when treated with Igf2 protein. Cotreatment with anti-Igf1R antibody reduced Igf1R and Akt phosphorylation to levels equal or below baseline in PZp53^{MED} cells. Phospho-Igf1R was detected by immunoprecipitation (*IP*) with anti-phosphotyrosine antibody and immunoblotting with anti-Igf1Rβ antibody. *C,* anti-Igf1R antibody inhibits MB cell, but not control cell (*HELA*), proliferation in a dose-dependent manner. Antibody was added for 48 h at the specified concentrations, and cell titer was determined. *D,* PZp53^{MED} cells were cotransfected with YFP and either a CFP control or sIgf2R. Cells were assessed for BrdUrd staining after 36 h (BrdUrd was added for the final 6 h). The percentage of YFP-positive cells that were also BrdUrd positive was calculated for each sample. *Columns,* mean; *bars,* SD.

leading to formation of early MBs. Most of these lesions resolve or remain as benign lesions that are noted in most asymptomatic adult *ptc1*+/− mice. In an ill-fated subset of these mice, the pre-MB cells would undergo additional changes, the most critical being those that cause increased transcription of *igf2*. Increased autocrine Igf2 production would allow persistence of these lesions and their conversion to a malignant phenotype. Such a further transformation would be consistent with the effects of Igf2 on cell survival and growth. These lesions then progress to form the advanced MB seen in ∼15% of *ptc1*+/− mice.

Given the apparent requirement of *igf2* for progression to advanced MB, it is notable that when *igf2* expression is analyzed in independent early MBs (Fig. 1*C*), a significant increase in *igf2* transcript is observed in ∼20% of lesions. This frequency is similar to the ∼15% of mice that form advanced MB, suggesting that those early MBs that have induced *igf2* transcription comprise the subset of lesions that will progress to advanced MB. Failure to induce *igf2* transcription would cause these lesions to regress or remain benign. In summary, Igf2 may be an important malignancy associated factor required for the progression to advanced MB, making it an attractive therapeutic target.

Igf2 as a therapeutic target in MB. Strategies for blocking Igf2 signaling for the treatment of human tumors, such as MB, might include inhibition of Igf1R with small molecule inhibitors or receptor-blocking antibodies. Blocking Igf1R offers the advantage of preventing signaling by both Igf1 and Igf2, which stimulate the same signaling cascades. Whether Igf1 contributes to *ptc1*+/− MB formation is unclear. Increased *igf1* expression is noted sporadically in *ptc1*+/− MBs (data not shown) but at levels much lower than those of *igf2*. We do not observe substitution for Igf2 by Igf1 in *igf2*−deficient *ptc1*+/− mice.

Our work shows the promise of specific targeting of the Igf2 ligand. We used a soluble Igf2R to inhibit MB cell proliferation, which presumably worked by sequestering Igf2. Recently, this same protein, produced from a transgene, was shown to inhibit tumor formation in a mouse model of intestinal adenoma associated with high Igf2 levels (31). Neutralizing antibodies specific to Igf2 could also achieve this end. Finally, manipulation of Igf-binding proteins (IgfBP) could block signaling by Igf ligands. For instance, IgfBP-3 can bind to and regulate the mitogenic activities of Igfs and inhibit their antiapoptotic effects (40).

Our data show a critical role for Igf2 in the progression and continued growth of MB in *ptc1*+/− mice. In human MB, dysregulation of the Shh pathway, often through loss of *PTCH*, is associated with a specific desmoplastic MB histology. Compared with classic MB, desmoplastic MBs have a distinct gene expression profile that includes increased expression of *igf2* and Shh target genes (41). It is possible that Igf2 could hold similar importance in this class of human MB and that Igf2-directed therapies could provide clinical benefit.

Disclosure of Potential Conflicts of Interest

No potential conflicts of interest were disclosed.

Acknowledgments

Received 6/10/2008; revised 7/24/2008; accepted 8/21/2008.

Grant support: National Cancer Institute grant #RO1 CA 088060. R.B. Corcoran and M.T. Barakat were supported by the Stanford Medical Scientist Training Program NIH training grant. T. Bachar Raveh was supported by a Damon Runyan postdoctoral fellowship. M.T. Barakat was also supported by a National Science Foundation graduate research fellowship. E.Y. Lee was supported by the NIH under Ruth L. Kirschstein National Research Service Award (5F32CA117775-03) from the National Cancer Institute. M.P. Scott is an investigator of the Howard Hughes Medical Institute.

The costs of publication of this article were defrayed in part by the payment of page charges. This article must therefore be hereby marked *advertisement* in accordance with 18 U.S.C. Section 1734 solely to indicate this fact.

We thank Drs. Argiris Efstratiadis and Jane Johnson for providing mouse strains, Dr. Susan McConnell for an *in situ* hybridization protocol, Dr. Bass Hassan for the sIgf2R plasmid, Dr. Anna Penn for RNA from Gli1- and Gli2-transfected fibroblasts, Natalia Snarskaya for assistance with microarray and reverse transcription-PCR experiments, and Hermie Manuel for assistance with mouse husbandry.

References

1. Goussia AC, Bruner JM, Kyritsis AP, Agnantis NJ, Fuller GN. Cytogenetic and molecular genetic abnormalities in primitive neuroectodermal tumors of the central nervous system. Anticancer Res 2000;20:65–73.
2. Raffel C, Jenkins RB, Frederick L, et al. Sporadic medulloblstomas contain PTCH mutations. Cancer Res 1997;57:842–5.
3. Johnson RL, Rothman AL, Xie J, et al. Human homolog of patched, a candidate gene for the basal cell nevus syndrome. Science 1996;272:1668–71.
4. Ingham PW, Taylor AM, Nakano Y. Role of the Drosophila patched gene in positional signaling. Nature 1991;353:184–7.
5. Goodrich LV, Johnson RL, Milenkovic L, McMahon JA, Scott MP. Conservation of the hedgehog/patched signaling pathway from flies to mice: induction of a mouse patched gene by Hedgehog. Genes Dev 1996;10: 301–12.
6. Marigo V, Johnson RL, Vortkamp A, Tabin CJ. Sonic hedgehog differentially regulates expression of GLI and GLI3 during limb development. Dev Biol 1996;180: 273–83.
7. Ruiz I Altaba A. Gli proteins encode context-dependent positive and negative functions: implications for development and disease. Development 1999;126: 3205–16.
8. Dahmane N, Ruiz i Altaba A. Sonic hedgehog regulates the growth and patterning of the cerebellum. Development 1999;126:3089–100.
9. Wallace VA. Purkinje-cell-derived Sonic hedgehog regulates granule neuron precursor cell proliferation in the developing mouse cerebellum. Curr Biol 1999;9: 445–8.
10. Wechsler-Reya RJ, Scott MP. Control of neuronal precursor proliferation in the cerebellum by Sonic Hedgehog. Neuron 1999;22:103–14.
11. Kenney AM, Rowitch DH. Sonic hedgehog promotes G(1) cyclin expression and sustained cell cycle progression in mammalian neuronal precursors. Mol Cell Biol 2000;20:9055–67.
12. Kenney AM, Cole MD, Rowitch DH. Nmyc upregulation by sonic hedgehog signaling promotes proliferation in developing cerebellar granule neuron precursors. Development 2003;130:15–28.
13. Oliver TG, Grasfeder LL, Carroll AL, et al. Transcriptional profiling of the Sonic hedgehog response: a critical role for N-myc in proliferation of neuronal precursors. Proc Natl Acad Sci U S A 2003;100:7331–6.
14. Goodrich LV, Milenkovic L, Higgins KM, Scott MP. Altered neural cell fates and medulloblastoma in mouse patched mutants. Science 1997;277:1109–13.
15. Hahn H, Wojnowski L, Zimmer AM, Hall J, Miller G, Zimmer A. Rhabdomyosarcomas and radiation hypersensitivity in a mouse model of Gorlin syndrome. Nat Med 1998;4:619–22.
16. Berman DM, Karhadkar SS, Hallahan AR, et al. Medulloblastoma growth inhibition by hedgehog pathway blockade. Science 2002;297:1559–61.
17. Romer JT, Kimura H, Magdaleno S, et al. Suppression of the Shh pathway using a small molecule inhibitor eliminates medulloblastoma in Ptc1(+/−)p53(−/−) mice. Cancer Cell 2004;6:229–40.
18. van Doorn J, Gilhuis HJ, Koster JG, et al. Differential patterns of insulin-like growth factor-I and -II mRNA expression in medulloblastoma. Neuropathol Appl Neurobiol 2004;30:503–12.
19. Chopra A, Brown KM, Rood BR, Packer RJ, MacDonald TJ. The use of gene expression analysis to gain insights into signaling mechanisms of metastatic medulloblastoma. Pediatr Neurosurg 2003;39:68–74.
20. Albrecht S, Waha A, Koch A, Kraus JA, Goodyer CG, Pietsch T. Variable imprinting of H19 and IGF2 in fetal cerebellum and medulloblastoma. J Neuropathol Exp Neurol 1996;55:1270–6.
21. Hahn H, Wojnowski L, Specht K, et al. Patched target Igf2 is indispensable for the formation of medulloblastoma and rhabdomyosarcoma. J Biol Chem 2000;275: 28341–4.
22. Zhan S, Shapiro D, Zhan S, et al. Concordant loss of imprinting of the human insulin-like growth factor II gene promoters in cancer. J Biol Chem 1995;270: 27983–6.
23. Rao G, Pedone CA, Valle LD, Reiss K, Holland EC, Fults DW. Sonic hedgehog and insulin-like growth factor signaling synergize to induce medulloblastoma formation from nestin-expressing neural progenitors in mice. Oncogene 2004;23:6156–62.
24. Hartmann W, Koch A, Brune H, et al. Insulin-like Growth Factor II is involved in the proliferation control of medulloblastoma and its cerebellar precursor cells. Am J Pathol 2005;166:1153–62.
25. Ingram WJ, Wicking CA, Grimmond SM, Forrest AR, Wainwright BJ. Novel genes regulated by Sonic Hedgehog in pluripotent mesenchymal cells. Oncogene 2002; 21:8196–205.
26. Lumpkin EA, Collisson T, Parab P, et al. Math1-driven GFP expression in the developing nervous system of transgenic mice. Gene Expr Patterns 2003;3:389–95.
27. Jensen P, Smeyne R, Goldowitz D. Analysis of cerebellar development in math1 null embryos and chimeras. J Neurosci 2004;24:2202–11.
28. Lee Y, Miller HL, Jensen P, et al. A molecular fingerprint for medulloblastoma. Cancer Res 2003;63: 5428–37.
29. Oliver TG, Read TA, Kessler JD, et al. Loss of patched and disruption of granule cell development in a pre-neoplastic stage of medulloblastoma. Development 2005;132:2425–39.
30. Zaina S, Newton RV, Paul MR, Graham CF. Local reduction in organ size in transgenic mice expressing a soluble Insulin-like Growth Factor II/Mannose-6-Phosphate Receptor. Endocrinology 1998;139:3886–95.
31. Harper J, Burns JL, Foulstone EJ, Pignatelli M, Zaina S, Hassan AB. Soluble IGF2 receptor rescues Apc(Min/+) intestinal adenoma progression induced by Igf2 loss of imprinting. Cancer Res 2006;66:1940–8.
32. Svaren J, Ehrig T, Abdulkadir SA, Ehrengruber MU, Watson MA, Milbrandt J. EGR1 target genes in prostate carcinoma cells identified by microarray analysis. J Biol Chem 2000;275:38524–31.
33. Hodzic D, Frey B, Marechal D, Scarcez T, Grooteclaes M, Winkler R. Cloning of breakpoints in and downstream the IGF2 gene that are associated with overexpression of IGF2 transcripts in colorectal tumours. Oncogene 1999;18:4710–7.
34. Li X, Kogner P, Sandstedt B, Haas OA, Ekstrom TJ. Promoter-specific methylation and expression alterations of igf2 and h19 are involved in human hepatoblastoma. Int J Cancer 1998;75:176–80.
35. Kang-Park S, Lee YI, Lee YI. PTEN modulates insulin-like growth factor II (IGF-II)-mediated signaling; the protein phosphatase activity of PTEN downregulates IGF-II expression in hepatoma cells. FEBS Lett 2003;545: 203–8.
36. Yao R, Cooper GM. Growth factor-dependent survival of rodent fibroblasts requires phosphatidylinositol 3-kinase but is independent of pp70S6K activity. Oncogene 1996;13:343–51.
37. Kenney AM, Widlund HR, Rowitch DH. Hedgehog and PI-3 Kinase signaling converge on Nmyc1 to promote cell cycle progression in cerebellar neuronal precursors. Development 2004;131:217–28.
38. Browd SR, Kenney AM, Gottfried ON, et al. N-myc can substitute for Insulin-like Growth Factor signaling in a mouse model of Sonic Hedgehog-induced medulloblastoma. Cancer Res 2006;66:2666–72.
39. Dudek H, Datta SR, Franke TF, et al. Regulation of neuronal survival by the serine-threonine protein kinase Akt. Science 1997;275:661–5.
40. Nickerson T, Huynh H, Pollak M. Insulin-like growth factor binding protein-3 induces apoptosis in MCF7 breast cancer cells. Biochem Biophys Res Commun 1997;237:690–3.
41. Pomeroy SL, Tamayo P, Gaasenbeek M, et al. Prediction of central nervous system embryonal tumour outcome based on gene expression. Nature 2002;415: 436–42.